CORNEA

Enhanced morphological assessment based on interocular asymmetry analysis for keratoconus detection

Ruilan Dong[1,2,3] · Yan Liu[1,2,3] · Yu Zhang[1,2,3] · Yueguo Chen[1,2,3]

Abstract

Purpose To clarify the interocular asymmetry of corneal morphological descriptors and evaluate its discriminant ability of keratoconus (KC).

Methods This retrospective study recruited 344 normal participants and 290 KC patients, randomized to training and validation datasets. Interocular correlation and agreement were evaluated on 44 corneal morphological descriptors derived from Schiempflug tomography. Logistic regression models were constructed using binocular data and of which diagnostic performance was evaluated using the area under receiver operating characteristics curve (AUC), net reclassification improvement (NRI), and integrated discrimination improvement (IDI).

Results Interocular agreement of corneal descriptors is better in the normal than in KC except for dimensions of cornea and anterior chamber. The interocular asymmetry increases along with the severity of KC. Interocular asymmetry in maximum anterior keratometry, mean anterior keratometry and higher-order aberrations of anterior surface show high AUC above 0.950. Binocular logistic regression index reaches an AUC of 0.963 with high specificity (95.2%) and brings gain to monocular parameters in distinguishing the normal eyes from KC (NRI = 0.080 (0.042 ~ 0.118), $P < 0.001$) and IDI = 0.071 (0.049 ~ 0.092), $P < 0.001$). Interocular asymmetry benefits even more in subclinical keratoconus (SKC) detection reflected by NRI (0.4784 (0.2703–0.6865), $P < 0.001$) and IDI (0.2680 (0.1495–0.3866), $P < 0.001$) measures.

Conclusion Interocular asymmetry is a well-characterized feature of KC and related to the severity. It is feasible to apply the interocular asymmetry in diagnosis of KC and SKC as a replenishment of monocular parameters and in progression tracking.

Keywords Keratoconus · Interocular asymmetry · Diagnostic model · Logistic regression · Schiempflug tomography

---

Key messages

What is known:

- The interocular asymmetry in keratometry, pachymetry and elevation of patients with keratoconus (KC) is significantly higher than that of normal individuals, and the degree of interocular asymmetry increases with the severity of KC.

- A small number of studies have shown diagnostic value of interocular asymmetry in keratometry and elevation for KC detection but few diagnostic models based on interocular asymmetry have been established.

What is new:

- The different expression of interocular asymmetry between the normal and KC, as well as its variation with the severity of KC, also exist in aberrations.

- This research constructs a well-performed combining model of interocular asymmetry for diagnosis of KC and confirms its additive value after being added into the monocular based model. The gain value of interocular asymmetry is even more prominent in the diagnosis of subclinical keratoconus (SKC).

Extended author information available on the last page of the article

Introduction

Early and precise diagnosis of keratoconus (KC) is crucial to assure safety of corneal refractive surgery and improve prognosis of KC by early treatment. The development of corneal topography and tomography system, corneal biomechanical examinations, and optical coherence tomography has provided us detailed data of the subtle progression of KC. However, a huge amount of corneal descriptors could be a burden for quick accurate diagnosis in the consulting room. Machine learning, as a branch of artificial intelligence, is exactly suitable to synthesize abundant data beyond the ability of humans [1]. Thus, there is a growing volume of machine learning research being conducted in KC detection over the past years [2]. Though gratifying diagnostic ability superior to junior doctors has been achieved [3], the machine learning model is still not precise enough especially for subclinical keratoconus (SKC) detection. There is still a need for exploring other auxiliary diagnostic indicators for improvement of current diagnostic models.

The corneal morphology has been proved to have good interocular correlation and symmetry in a normal individual, which provided theoretical basis for the construction of corneal transplantation substitutes [4–6]. In fact, the study of interocular asymmetry can also facilitate the diagnosis of KC, which is a bilateral but asymmetric non-inflammatory disease. However, although interocular asymmetry is a typical character in KC, only a few studies have quantitatively analyzed the range in patients with KC [7–10]. The existing classic diagnostic indicators are all independently based on monocular data, in lack of an overall evaluation of interocular linkage [11–13]. Whether the interocular asymmetry in morphological parameters has diagnostic significance and how to determine the cutoff value for distinguishing the normal from KC are questions worthy of discussion.

This study attempts to clarify the range of interocular asymmetry of corneal descriptors in the normal and keratoconic eyes, and to explore the feasibility of applying it to the diagnosis of KC.

Materials and methods

Study design

This is a retrospective chart review study. Participants who had undergone refractive surgery or been diagnosed as KC in Peking University Institute of Laser Medicine from January 2016 to January 2021 were consecutively recruited. The protocol was adhered to the Declaration of Helsinki and approved by the Institutional Review Board of the Peking University Third Hospital (2023-250-01). The informed consent was obtained from all subjects prior to data collection.

Study population and data collection

Each participant underwent complete ophthalmic examinations, including subjective and cycloplegic refraction, intraocular pressure measurement, slit-lamp biomicroscopy examination, corneal tomography (Pentacam HR, Oculus GmbH, Wetzlar, Germany), and biomechanical examination (Corvis, Oculus GmbH, Wetzlar, Germany). The Pentacam HR and Corvis were calibrated periodically by the manufacturer and operated by a same trained technician. Poor quality exams were discarded and recaptured, only qualified pre-operative reports graded as "OK" (defined by manufacturer) were adopted.

For the normal group, the inclusion criteria were eyes showing normal values in the standardized indicies (less than 1.6 for all kinds of deviation of normality), with stable refractive status for at least 2 years after refractive surgery. The KC group was diagnosed and included in accordance with the global consensus on KC diagnosis [14] by two experienced ophthalmologists (YGC and YZ) using the comprehensive results of ophthalmic examinations. Diagnosis is considered on a human unit basis. As long as one eye of whom is diagnosed as keratoconus (with abnormal standardized indicies), the patient will be included in the keratoconus group. Therefore, unilateral keratoconus and early bilateral keratoconus patients with temporarily unilateral involvement were all included. The exclusion criteria were previous ocular trauma or surgery, coexisting ocular disease except for ametropia, chronic use of topical medication, and wearing corneal contact lenses in 3 weeks before the examination. The two groups were randomly divided into two datasets (training and validation) in a 7:3 ratio. Besides, we referred to previous studies and considered patients with Keratoconus Severity Score (KSS) 0–2 in KC group as SKC [15–17]. Data of the SKC group did not independently participate in model training and was only used separately during validation to explore the possibility of applying the models for SKC diagnosis.

Statistical analysis

Interocular asymmetry was defined as the absolute value of the right eye minus the left eye. The KC severity grading was based on the KSS output by Pentacam HR [18]. The normality was assessed using Kolmogorov–Smirnov test and the data were expressed accordingly. Spearman's coefficients

and intraclass correlation coefficients (ICC) were computed to analyze the interocular correlation and agreement. A *t* test or Mann-Whitney *U* test was used to compare the interocular difference values between the normal and keratoconic eyes. A one-way ANOVA or Kruskal-Wallis *H* test was used to compare the interocular asymmetry among KC subgroups divided by disease severity. The logistic regression was performed on the variables screened by lasso to construct monocular logistic regression index (MLRI) and binocular logistic regression index (BLRI) using right eye data and interocular difference values, respectively. Furthermore, a binocular-assisted logistic regression index (BaLRI) was constructed by introducing BLRI into MLRI. The receiver operating characteristic (ROC) curve was drawn to evaluate the diagnostic ability of the interocular asymmetry of corneal tomographic parameters and the combination of them. Differences in the area under the receiver operating characteristic curve (AUC) of the logistic models constructed in current study and Belin/Ambrósio deviation (BAD-D) were compared using Delong's test. Net reclassification improvement (NRI) and integrated discrimination improvement (IDI) were also estimated to evaluate the additive value of BLRI in predicting KC. Statistical analysis was performed using SPSS 24.0 (IBM Corporation, Armonk, NY, USA) and R software 4.2.2 (R Foundation for Statistical Computing, Vienna, Austria). A *P* value of <0.05 was regarded as statistically significant.

Results

Demographic characteristics

A total of 344 normal subjects and 290 KC patients were enrolled in the statistics. The mean age is 27.92 ± 7.09 and 24.86 ± 6.20 in the normal and KC group, respectively. One hundred thirty-seven (39.83%) participants in the normal group and 198 (68.28%) patients in the KC group are male. Both the mean age and the sex ratio are significantly different between the two groups (*P*<0.001, Table 1). The spherical equivalent (SE) and the best corrected visual acuity (BCVA) are significantly higher in the KC group than those in the normal group (*P*<0.001, Table 1). The training dataset included 231 normal participants and 213 KC, whereas the validation dataset consisted of 113 normal participants and 77 KC. The demographic characteristics of the two datasets are summarized in Table 1.

Interocular consistency

The corneal descriptors of both groups are listed in Table 2. Almost all descriptors in the normal group have moderate to high (ICC>0.6, *P*<0.001, Table 2) interocular agreement

except for Chord Mu, differential pachymetry between the corneal apex and the thinnest point, horizontal deviation of maximum keratometry and the thinnest point, and coma of both anterior and posterior surfaces with relatively weak interocular agreement. However, in the KC group, the ICC for most descriptors was less than 0.6 suggesting weak or poor interocular agreement (Table 2).

Interocular asymmetry and keratoconus grade

The ranges of interocular asymmetry are shown in Table 3. The interocular asymmetry of all descriptors in the KC group were higher than those in the normal group (*P*<0.001, Table 3). Besides, the subgroup analysis of the KC group showed that the interocular asymmetry gradually increased as the severity of KC increased (Table 3, Fig. 1).

Diagnostic performance of interocular asymmetry and logistic models

The logistic regression produced the following formula: BLRI = EXP (Beta)/(1+ EXP (Beta)), where Beta=B1 × steep anterior keratometry (K2 (F)) +B2 × maximum anterior keratometry (K Max (F)) +B3 × vertical deviation of the point of maximum anterior keratometry (K Max Y) + B4 × steep posterior keratometry (K2 (B)) + B5 × pachymetry at the pupil center (Pachy Pupil) + B6 × eccentricity in 9-mm zone (EccSph) + B7 × back elevation at thinnest point (B.Ele.Th) + B8 and B1 = 3.175, B2 = 0.453; B3 = −1.042, B4 = 1.041, B5 = 0.978, B6 = −0.277, B7 = 0.835, B8 = 1.679.

The diagnostic performance of the interocular asymmetry and the logistic regression indices are shown in Table 4 and Fig. 2. The AUC of interocular asymmetry in mean anterior keratometry, maximum anterior keratometry, root mean square of whole cornea aberrations, and of higher-order aberrations of posterior surface exceeds 0.950 in discriminating KC from the normal eyes. A cutoff value of 0.303 for the BLRI reaches the AUC of 0.9633, with 93.0% sensitivity and 95.2% specificity. The AUC was 0.9626 for the MLRI with lower sensitivity (92.5%) and specificity (93.5%). The BaLRI reaches the highest AUC of 0.971 with higher sensitivity (95.3%) and specificity (97.0%) than BLRI and MLRI. Though the Delong's test reported no significant difference among the three models, the interocular asymmetry improved the NRI (0.0798 (0.0415 – 0.1180), *P* < 0.001) and IDI (0.0707 (0.0491 – 0.0922), *P* < 0.001), indicating significant improvement in discriminatory power for KC after adding interocular asymmetry to the established monocular model. In the validation, the BaLRI also achieved the highest AUC of 0.9844 and correctly classified 98.4%

Table 1 Demographic characteristics in the both groups of different datasets

	Training dataset (n=444) Normal (n=231)	Training dataset KC (n=213)	Validation dataset (n=190) Normal (n=113)	Validation dataset KC (n=77)	Combined dataset (n=634) Normal (n=344)	Combined dataset KC (n=290)	P^a
Age (years)	28.07 ± 6.99; 27.63 (21.69, 33.07)	24.92 ± 6.36; 24.59 (21.05, 29.22)	27.61 ± 7.29; 26.58 (21.44, 32.28)	24.70 ± 5.78; 25.32 (20.78, 27.64)	27.92 ± 7.09; 27.28 (21.66, 32.87)	24.86 ± 6.20; 24.61 (21.03, 28.84)	<0.001
Gender							
Female	139 (60.17%)	68 (31.92%)	68 (60.18%)	24 (31.17%)	207 (60.17%)	92 (31.72%)	<0.001
Male	92 (39.83%)	145 (68.08%)	45 (39.82%)	53 (68.83%)	137 (39.83%)	198 (68.28%)	
SE (D)							
OD	-5.50 (-7.00, -4.50)	-6.88 (-9.50, -4.88)	-5.50 (-6.63, -4.06)	-7.63 (-10.31, -4.50)	-5.50 (-6.84, -4.25)	-7.00 (-9.72, -4.78)	<0.001
OS	-5.50 (-6.75, -4.00)	-6.38 (-9.13, -4.50)	-5.25 (-6.69, -3.88)	-6.00 (-9.75, -4.31)	-5.38 (-6.75, -4.00)	-6.38 (-9.25, -4.50)	<0.001
BCVA							
OD	-0.08 (-0.08, -0.04)	0.22 (0.05, 0.40)	-0.08 (-0.08, -0.04)	0.22 (0.10, 0.43)	-0.08 (-0.08, -0.04)	0.22 (0.05, 0.40)	<0.001
OS	-0.04 (-0.08, -0.04)	0.17 (0.05, 0.40)	-0.04 (-0.08, -0.04)	0.15 (0.05, 0.30)	-0.04 (-0.08, -0.04)	0.15 (0.05, 0.40)	<0.001
Grading	OD / OS	OD / OS	OD / OS	OD / OS	OD / OS	OD / OS	
Normal	231 / 231	-	113 / 113	-	344 / 344	-	
KSS 1	-	98 / 102	-	33 / 39	-	131 / 141	
KSS 2	-	43 / 45	-	7 / 15	-	50 / 60	
KSS 3	-	61 / 50	-	29 / 18	-	90 / 68	
KSS 4	-	11 / 16	-	8 / 5	-	19 / 21	

SE, spherical equivalent; *D*, dioptor; *BCVA*, best corrected visual ability

[a] Mann-Whitney *U* test

Table 2 Summary of corneal descriptors in the normal and KC groups

	Normal (n=344)				KC (n=290)			
	OD	OS	ICC	P^a	OD	OS	ICC	P^a
Anterior surface								
K1 (D)	42.45 (41.70, 43.20)	42.40 (41.50, 43.20)	0.93 (0.92, 0.95)	<0.001	44.90 (42.98, 47.61)	44.60 (42.80, 46.90)	0.44 (0.30, 0.56)	<0.001
K2 (D)	43.60 (42.70, 44.50)	43.60 (42.70, 44.70)	0.91 (0.89, 0.93)	<0.001	48.00 (45.50, 51.50)	47.70 (44.88, 51.03)	0.33 (0.15, 0.46)	<0.001
Km (D)	43.00 (42.20, 43.90)	42.90 (42.13, 43.90)	0.93 (0.92, 0.95)	<0.001	46.30 (44.20, 49.40)	46.20 (43.70, 48.50)	0.37 (0.20, 0.50)	<0.001
K Max (D)	44.09 (43.08, 45.13)	44.16 (43.18, 45.30)	0.85 (0.81, 0.88)	<0.001	53.83 (48.13, 59.91)	52.28 (47.32, 58.27)	0.17 (−0.05, 0.34)	0.060
K Max X	−0.07 (−0.32, 0.07)	0.00 (−0.13, 0.14)	−0.26 (−0.56, −0.02)	0.985	0.07 (−0.13, 0.20)	−0.07 (−0.22, 0.13)	−0.50 (−0.89, −0.19)	1
K Max Y	0.07 (−0.91, 1.93)	−0.46 (−1.00, 1.96)	0.67 (0.59, 0.73)	<0.001	−0.96 (−1.46, −0.48)	−0.99 (−1.44, −0.53)	0.68 (0.59, 0.74)	<0.001
Asph. Q F	−0.31 (−0.38, −0.24)	−0.31 (−0.39, −0.24)	0.83 (0.79, 0.86)	<0.001	−0.70 (−1.05, −0.46)	−0.61 (−0.98, −0.41)	0.37 (0.20, 0.50)	<0.001
F.Ele.Th (µm)	2.00 (1.00, 3.00)	2.00 (1.00, 3.00)	0.66 (0.58, 0.73)	<0.001	18.00 (8.00, 26.75)	15.00 (8.00, 24.50)	0.23 (0.03, 0.39)	0.012
RMS (CF)	1.62 (1.31, 2.04)	1.72 (1.34, 2.18)	0.72 (0.65, 0.77)	<0.001	9.14 (4.75, 14.46)	8.45 (4.07, 12.90)	0.11 (−0.12, 0.29)	0.160
RMS HOA (CF)	0.35 (0.31, 0.41)	0.36 (0.31, 0.42)	0.73 (0.66, 0.78)	<0.001	2.10 (1.08, 3.24)	2.00 (0.91, 3.15)	0.24 (0.04, 0.40)	0.011
RMS LOA (CF)	1.57 (1.28, 1.99)	1.68 (1.30, 2.15)	0.72 (0.65, 0.77)	<0.001	8.92 (4.62, 14.03)	8.18 (3.97, 12.52)	0.11 (−0.13, 0.29)	0.172
Z 3 1 (CF)	−0.17 (−0.34, 0.06)	0.17 (−0.05, 0.39)	−0.61 (−0.67, −0.54)	1	−0.54 (−1.97, 0.20)	0.49 (−0.12, 2.27)	−0.70 (−1.14, −0.35)	1
Z 3 −1 (CF)	−0.04 (−0.37, 0.34)	−0.11 (−0.44, 0.31)	0.77 (0.72, 0.81)	<0.001	−4.46 (−7.95, −2.07)	−4.14 (−7.46, −1.42)	0.49 (0.36, 0.60)	<0.001
Z 4 0 (CF)	1.45 (1.30, 1.63)	1.45 (1.29, 1.61)	0.70 (0.63, 0.76)	<0.001	−0.19 (−1.93, 1.02)	0.22 (−1.53, 1.24)	0.20 (0.00, 0.37)	0.027
Posterior surface								
K1 (D)	−6.10 (−6.20, −5.90)	−6.00 (−6.20, −5.90)	0.89 (0.87, 0.91)	<0.001	−6.60 (−7.10, −6.10)	−6.45 (−6.90, −6.10)	0.44 (0.30, 0.56)	<0.001
K2 (D)	−6.40 (−6.60, −6.20)	−6.40 (−6.60, −6.20)	0.89 (0.86, 0.91)	<0.001	−7.30 (−8.00, −6.70)	−7.10 (−7.80, −6.60)	0.39 (0.23, 0.52)	<0.001
Km (D)	−6.20 (−6.40, −6.10)	−6.20 (−6.40, −6.00)	0.90 (0.88, 0.92)	<0.001	−6.90 (−7.40, −6.50)	−6.80 (−7.30, −6.30)	0.40 (0.24, 0.52)	<0.001
Asph. Q B	−0.32 (−0.40, −0.23)	−0.32 (−0.40, −0.24)	0.86 (0.83, 0.89)	<0.001	−0.74 (−1.11, −0.46)	−0.65 (−1.00, −0.37)	0.46 (0.32, 0.57)	<0.001
B.Ele.Th (µm)	4.00 (2.00, 6.00)	4.00 (2.00, 6.00)	0.76 (0.70, 0.80)	<0.001	39.00 (22.00, 58.00)	37.00 (20.00, 53.50)	0.36 (0.20, 0.49)	<0.001
RMS (CB)	0.81 (0.71, 0.92)	0.87 (0.77, 0.98)	0.74 (0.68, 0.79)	<0.001	2.25 (1.37, 3.46)	2.19 (1.31, 3.30)	0.24 (0.05, 0.40)	0.010
RMS HOA (CB)	0.18 (0.17, 0.20)	0.19 (0.17, 0.21)	0.77 (0.71, 0.81)	<0.001	0.59 (0.37, 0.87)	0.57 (0.35, 0.84)	0.29 (0.11, 0.44)	0.002
RMS LOA (CB)	0.78 (0.69, 0.89)	0.86 (0.75, 0.96)	0.74 (0.68, 0.79)	<0.001	2.15 (1.28, 3.37)	2.10 (1.26, 3.15)	0.24 (0.04, 0.40)	0.010
Z 3 1 (CB)	−0.13 (−0.49, 0.15)	0.05 (−0.29, 0.41)	−0.50 (−0.58, −0.42)	1	−1.21 (−4.65, 0.26)	0.87 (−0.40, 4.66)	−0.35 (−1.62, −0.65)	1
Z 3 −1 (CB)	0.43 (−0.16, 1.05)	0.20 (−0.34, 0.86)	0.80 (0.75, 0.84)	<0.001	−9.74 (−16.78, −4.42)	−8.99 (−15.59, −3.07)	0.57 (0.45, 0.66)	<0.001
Z 4 0 (CB)	3.65 (3.25, 4.06)	3.70 (3.26, 4.12)	0.75 (0.68, 0.79)	<0.001	−0.77 (−5.13, 1.84)	0.12 (−3.49, 2.91)	0.31 (0.12, 0.45)	0.001
Whole cornea								
TCT (µm)	546.00 (526.00, 565.00)	547.00 (527.00, 567.00)	0.98 (0.97, 0.98)	<0.001	462.00 (433.38, 494.25)	464.50 (433.75, 496.25)	0.78 (0.73, 0.83)	<0.001
Pachy Apex (µm)	550.00 (529.25, 568.75)	551.50 (531.00, 571.00)	0.98 (0.98, 0.98)	<0.001	468.00 (441.00, 503.00)	474.50 (443.00, 504.00)	0.78 (0.72, 0.82)	<0.001
CCT (µm)	549.50 (530.00, 570.00)	552.00 (532.00, 571.75)	0.98 (0.98, 0.99)	<0.001	475.50 (453.00, 509.00)	482.00 (450.00, 510.25)	0.84 (0.80, 0.87)	<0.001
differential pachymetry (µm)	4.00 (2.00, 5.00)	4.00 (2.00, 5.00)	0.58 (0.48, 0.66)	<0.001	7.00 (4.00, 10.00)	7.00 (4.00, 11.00)	0.64 (0.55, 0.72)	<0.001

Table 2 (continued)

	Normal (n=344)				KC (n=290)			
	OD	OS	ICC	P^a	OD	OS	ICC	P^a
Chord_Mu (mm)	0.16 (0.11, 0.24)	0.16 (0.09, 0.24)	0.52 (0.40, 0.61)	<0.001	0.31 (0.17, 0.45)	0.32 (0.20, 0.44)	0.45 (0.25, 0.60)	<0.001
PachyMinX	−0.47 (−0.62, −0.28)	0.40 (0.26, 0.55)	−0.61 (−0.67, −0.54)	1	−0.39 (−0.54, −0.24)	0.40 (0.23, 0.54)	−0.39 (−0.48, −0.29)	1
PachyMinY	−0.44 (−0.61, −0.33)	−0.52 (−0.67, −0.35)	0.78 (0.73, 0.82)	<0.001	−0.47 (−0.65, −0.33)	−0.54 (−0.73, −0.35)	0.57 (0.46, 0.66)	<0.001
PupilX	0.01 (−0.08, 0.11)	−0.02 (−0.11, 0.06)	−0.62 (−0.68, −0.55)	1	0.02 (−0.10, 0.12)	−0.03 (−0.12, 0.09)	−0.43 (−0.51, −0.33)	1
PupilY	0.09 (0.01, 0.17)	0.08 (−0.01, 0.17)	0.63 (0.54, 0.70)	<0.001	0.27 (0.10, 0.41)	0.26 (0.09, 0.43)	0.59 (0.48, 0.67)	<0.001
EccSph	0.54 (0.47, 0.60)	0.54 (0.47, 0.61)	0.90 (0.88, 0.92)	<0.001	0.86 (0.67, 1.04)	0.82 (0.63, 1.00)	0.42 (0.27, 0.54)	<0.001
RMS (Cornea)	1.38 (1.08, 1.78)	1.43 (1.12, 1.92)	0.71 (0.64, 0.76)	<0.001	8.01 (3.95, 12.63)	7.21 (3.47, 11.43)	0.10 (−0.13, 0.29)	0.178
RMS HOA (Cornea)	0.34 (0.29, 0.41)	0.36 (0.30, 0.42)	0.70 (0.63, 0.76)	<0.001	1.81 (0.90, 2.83)	1.81 (0.78, 2.76)	0.23 (0.03, 0.39)	0.015
RMS LOA (Cornea)	1.33 (1.02, 1.74)	1.38 (1.05, 1.87)	0.71 (0.64, 0.76)	<0.001	7.83 (3.84, 12.29)	7.07 (3.38, 11.16)	0.10 (−0.14, 0.28)	0.189
C.Height (mm)	3.21 (3.05, 3.39)	3.22 (3.04, 3.38)	0.98 (0.98, 0.99)	<0.001	3.33 (3.15, 3.53)	3.33 (3.15, 3.54)	0.94 (0.93, 0.96)	<0.001
C.Volume (mm³)	187.20 (169.45, 209.90)	190.15 (170.73, 214.15)	0.98 (0.97, 0.98)	<0.001	192.35 (169.95, 212.48)	191.25 (172.08, 214.65)	0.97 (0.96, 0.98)	<0.001
Cor.Vol. (mm³)	61.20 (59.00, 63.40)	61.30 (59.10, 63.50)	0.98 (0.98, 0.99)	<0.001	56.85 (54.28, 59.03)	57.15 (54.6, 59.40)	0.97 (0.97, 0.98)	<0.001
Cornea Dia. (mm)	11.70 (11.40, 11.95)	11.70 (11.40, 12.00)	0.95 (0.94, 0.96)	<0.001	11.70 (11.40, 12.00)	11.70 (11.50, 12.03)	0.93 (0.91, 0.95)	<0.001
Density (%)	13.30 (12.50, 14.00)	13.15 (12.50, 13.88)	0.92 (0.91, 0.94)	<0.001	12.80 (11.80, 14.00)	12.85 (11.90, 13.90)	0.94 (0.93, 0.96)	<0.001
BAD D	0.83 (0.45, 1.16)	0.85 (0.49, 1.19)	0.83 (0.79, 0.86)	<0.001	7.07 (3.97, 10.53)	6.48 (3.63, 9.82)	0.30 (0.12, 0.44)	0.001

K1, flat keratometry; K2, steep keratometry; Kn, mean keratometry; K Max, maximum keratometry; F.Ele.Th/B.Ele.Th, front/back elevation in thinnest location; RMS, root mean square; HOA, high-order aberration; LOA, low-order aberration; C.Height, anterior chamber depth measured from the posterior corneal surface to the ocular lens in apex position; C.Volume, anterior chamber volume in mm³ at a diameter of 10 mm around the apex; Cor.Vol., anterior chamber volume in mm³ at a diameter of 10 mm around the apex; Cornea Dia., corneal diameter; BAD-D, Belin/Ambrósio deviation

^{a}p for ICC

of the cases from the normal. The BaLRI showed a trend of even higher AUC than that of BAD-D in distinguishing SKC from normal eyes, though not significantly different (0.975 vs 0.970, P=0.6363). The interocular asymmetry improved the NRI (0.4784 (0.2703 – 0.6865), $P < 0.001$) and IDI (0.2680 (0.1495 – 0.3866), $P < 0.001$) measures for SKC detection to a greater extent than those in KC detection. The BaLRI has also shown good performance in diagnosing different grades of keratoconus, with AUC above 0.97 for KSS grades 1–4 (Table 5 and Fig. 3).

Discussion

In the present study, we compared the interocular correlations in the normal and KC populations, and our findings are generally consistent with the previous researches. Henriquez et al. [19] focused on pachymetric data and reported the ICC was significantly higher in the normal eyes (0.96, 0.96, and 0.85 for central corneal thickness (CCT), pachymetry at the thinnest point (TP), and posterior elevation at the thinnest point of the cornea (PETP), respectively) than in the KC eyes (0.73, 0.64, and 0.39 for CCT, TP, and PETP, respectively). Naderan et al. [20] additionally evaluated the keratometry in both anterior and posterior corneal surfaces and refraction among the normal, keratoconus suspect (KCS), and KC groups. The intraclass agreement was poor in patients with KC, but moderate to good in patients with KCS, and strong in the normal group. Our study further expanded the scope of evaluation, and observed good interocular consistency in the corneal diameter, volume, density, and anterior chamber depth in both normal and KC eyes. While considering corneal curvature, thickness, elevation, asphericity, and aberration, good to strong intraclass correlations only existed in normal participants, but weak to poor in KC patients. In contrast to our study, Dienes et al. [21] reported good interocular correlations in posterior elevation and pachymetry in both groups with correlation coefficients greater than 0.6. Mehlan et al. [22] reported that the mean ICC of CCT, TP, and PETP is high in both normal (0.74–0.86) and KC group (0.73–0.83) as well. We supposed that maybe more patients with mild KC were included in the aforementioned two studies, of whom the interocular asymmetry could be relatively small even in the KC eyes. Detailed data were needed to further compare and analyze the disagreement.

The ranges of interocular asymmetry obtained in this study are basically the same as those in the previous studies [19–21, 23, 24], and some parameters that have not been evaluated ever before are complemented. A greater interocular asymmetry was observed in most corneal descriptors except for corneal diameter in the KC patients than in normal participants. Galletti et al. [25] carried out subgroup analysis on the anisometropia population in the normal group, and

the results showed that the anisometropia patients still have good corneal morphological symmetry. This indicates that interocular asymmetry tends to have certain specificity in KC, and comparative evaluation of both eyes may be valuable for the diagnosis of early KC.

We also noted that the interocular asymmetry is positively related to the severity, though different grading standards of severity were adopted in relevant researches. Some used single parameters to evaluate the severity of KC [9, 21, 24, 25]. Galletti et al. [25] reported a positive relationship between the steepest (of both eyes) mean anterior keratometry and the interocular asymmetry in keratometry and front elevation at thinnest point. Dienes [21] and Bussieres [24] found obvious relationship between interocular asymmetry of single biomechanics and biomechanics itself in mean K, steep K, CCT, thinnest corneal thickness (TCT), and posterior elevation (PE).

However, although single indices representing the severity of the disease had obtained positive results, the indices graded by comprehensive consideration of different morphological dimensions should be more objective on reflecting the impact of severity on interocular asymmetry. Thus, some studies included the present one adopted widely accepted grading parameters or systems, including Keratoconus Severity Index (KSI), Amsler–Krumeich classification, KSS and Topographical Keratoconus Classification (TKC) [10, 20, 25, 26]. As anticipated, the range of interocular asymmetry increased with the grade of the worse eye. In the present study, the KC group was divided into four subgroups according to the comprehensive grading parameter KSS. The interocular asymmetry in the normal group was significantly smaller than each of the severer three subgroups in most corneal parameters, while was smaller than the mildest KC group only in partial indices relating to keratometry, pachymetry, and elevation, which provides a clue of more sensitive parameters in diagnosing SKC.

Besides, Bussieres et al. [24] further divided the KC participants into asymmetric and symmetric subgroups, based on the standards that the interocular asymmetry in the mean K, flat K, and steep K should be equal to or less than 2.5 D and in the TCT ≤25.0 μm. Significant differences were found in the parameters mentioned above among the two subgroups and the normal one. We hold that the so-called symmetrical KC subgroup might be relatively mild KC, considering that this group has smaller mean K and thicker pachymetry at the apex of cornea than the asymmetrical KC subgroup. Therefore, the intergroup difference might be a manifestation of the increase of asymmetry with the severity.

Eppig et al. [26] even included the biomechanical parameters into analysis and found the interocular asymmetry in biomechanical parameters are negatively related to the severity as well at KC stages 0 to 3. However, an inverse alteration

Table 3 Comparisons of interocular asymmetry between the normal and KC groups

	Normal (n=344)	KC (n=290)	P^a	KC (n=290)				P^b
				KSS 1 (n=16)	KSS 2 (n=100)	KSS 3 (n=136)	KSS 4 (n=38)	
Anterior surface								
K1 (D)	0.20 (0.10, 0.40)	2.50 (0.90, 4.83)	<0.001	0.45 (0.13, 0.95)	1.30 (0.53, 2.60)	3.00 (1.43, 5.70)	6.80 (3.73, 9.90)	<0.001
K2 (D)	0.20 (0.10, 0.40)	3.80 (2.00, 6.80)	<0.001	1.05 (0.63, 1.90)	2.85 (1.60, 4.47)	4.45 (2.53, 7.68)	9.10 (4.38, 11.15)	<0.001
Km (D)	0.20 (0.10, 0.30)	3.00 (1.30, 5.50)	<0.001	0.70 (0.30, 0.98)	2.05 (1.10, 3.28)	3.65 (1.80, 6.35)	7.80 (3.68, 10.50)	<0.001
K Max (D)	0.28 (0.13, 0.51)	7.11 (3.45, 12.85)	<0.001	2.37 (1.70, 3.28)	5.26 (3.20, 7.86)	8.47 (4.43, 13.62)	14.21 (9.59, 18.43)	<0.001
K Max X	0.26 (0.12, 0.69)	0.35 (0.14, 0.67)	0.087	0.56 (0.23, 1.01)	0.32 (0.18, 0.74)	0.33 (0.13, 0.61)	0.46 (0.14, 0.64)	0.158
K Max Y	0.56 (0.23, 1.72)	0.45 (0.21, 0.79)	<0.001	0.48 (0.29, 0.92)	0.37 (0.19, 0.69)	0.39 (0.19, 0.75)	0.68 (0.37, 0.89)	<0.001
Asph. Q F	0.03 (0.02, 0.06)	0.33 (0.15, 0.64)	<0.001	0.11 (0.03, 0.22)	0.24 (0.12, 0.43)	0.41 (0.21, 0.72)	0.85 (0.44, 1.09)	<0.001
F.Ele.Th (μm)	1.00 (0.00, 1.00)	11.00 (6.00, 19.00)	<0.001	3.50 (2.25, 6.00)	8.00 (4.00, 11.00)	13.00 (7.00, 21.00)	23.00 (14.75, 28.00)	<0.001
RMS (CF)	0.22 (0.09, 0.37)	6.07 (2.55, 9.49)	<0.001	2.24 (1.37, 2.53)	4.04 (2.31, 6.36)	7.63 (3.40, 11.60)	9.23 (7.34, 16.04)	<0.001
RMS HOA (CF)	0.04 (0.02, 0.07)	1.31 (0.59, 2.14)	<0.001	0.50 (0.28, 0.60)	0.91 (0.55, 1.48)	1.75 (0.68, 2.63)	2.28 (1.69, 3.51)	<0.001
RMS LOA (CF)	0.22 (0.09, 0.37)	5.91 (2.48, 9.29)	<0.001	2.16 (1.33, 2.46)	3.98 (2.31, 6.22)	7.37 (3.39, 11.29)	8.96 (7.18, 15.66)	<0.001
Z 3 1 (CF)	0.45 (0.22, 0.73)	1.99 (0.74, 4.38)	<0.001	0.71 (0.22, 1.15)	1.48 (0.73, 2.94)	2.82 (0.85, 5.62)	3.25 (1.03, 6.28)	<0.001
Z 3 -1 (CF)	0.25 (0.10, 0.46)	2.77 (1.22, 5.18)	<0.001	1.22 (0.49, 1.78)	2.01 (0.90, 3.50)	3.52 (1.46, 6.72)	6.13 (2.46, 8.50)	<0.001
Z 4 0 (CF)	0.09 (0.04, 0.18)	1.65 (0.64, 3.15)	<0.001	0.38 (0.14, 0.52)	0.99 (0.48, 2.11)	2.19 (0.95, 3.89)	3.53 (2.31, 6.23)	<0.001
Posterior surface								
K1 (D)	0.10 (0.00, 0.10)	0.50 (0.20, 1.00)	<0.001	0.15 (0.10, 0.20)	0.30 (0.20, 0.60)	0.65 (0.30, 1.10)	1.20 (0.88, 1.70)	<0.001
K2 (D)	0.10 (0.00, 0.10)	0.70 (0.40, 1.30)	<0.001	0.20 (0.10, 0.38)	0.60 (0.30, 0.90)	0.85 (0.43, 1.39)	1.55 (0.80, 2.13)	<0.001
Km (D)	0.00 (0.00, 0.10)	0.60 (0.30, 1.10)	<0.001	0.10 (0.10, 0.28)	0.45 (0.23, 0.70)	0.70 (0.33, 1.20)	1.40 (0.80, 1.83)	<0.001
Asph. Q B	0.03 (0.02, 0.06)	0.36 (0.14, 0.65)	<0.001	0.13 (0.01, 0.18)	0.28 (0.10, 0.46)	0.38 (0.17, 0.72)	0.75 (0.39, 0.98)	<0.001
B.Ele.Th (μm)	1.00 (1.00, 2.00)	22.00 (10.50, 34.00)	<0.001	10.00 (6.00, 17.50)	15.50 (9.00, 25.00)	26.00 (11.00, 38.00)	38.00 (24.50, 51.50)	<0.001
RMS (CB)	0.08 (0.04, 0.13)	1.17 (0.55, 1.84)	<0.001	0.34 (0.27, 0.64)	0.85 (0.44, 1.33)	1.46 (0.63, 2.28)	2.14 (1.38, 3.32)	<0.001
RMS HOA (CB)	0.01 (0.01, 0.02)	0.29 (0.14, 0.46)	<0.001	0.13 (0.06, 0.15)	0.23 (0.10, 0.31)	0.35 (0.18, 0.58)	0.55 (0.30, 0.82)	<0.001
RMS LOA (CB)	0.08 (0.04, 0.13)	1.12 (0.54, 1.79)	<0.001	0.32 (0.25, 0.64)	0.81 (0.42, 1.26)	1.42 (0.63, 2.19)	2.07 (1.38, 3.22)	<0.001
Z 3 1 (CB)	0.59 (0.26, 1.03)	4.20 (1.64, 9.47)	<0.001	2.02 (0.19, 3.30)	2.94 (1.05, 6.69)	5.62 (2.04, 11.94)	5.28 (2.06, 12.78)	<0.001
Z 3 -1 (CB)	0.52 (0.22, 0.84)	5.27 (2.17, 9.82)	<0.001	3.00 (0.83, 5.14)	4.01 (0.99, 7.32)	6.23 (2.43, 11.51)	10.11 (3.09, 14.41)	<0.001
Z 4 0 (CB)	0.25 (0.12, 0.46)	3.93 (1.24, 6.79)	<0.001	0.62 (0.21, 2.14)	2.80 (0.95, 5.14)	4.57 (1.53, 8.51)	7.95 (4.28, 11.32)	<0.001
Whole cornea								
TCT (μm)	5.00 (2.00, 8.00)	26.00 (14.00, 39.00)	<0.001	18.00 (9.75, 19.75)	20.00 (11.25, 28.75)	30.25 (15.63, 45.00)	45.50 (29.00, 61.25)	<0.001
Pachy Apex (μm)	5.00 (2.00, 8.00)	27.00 (13.00, 41.00)	<0.001	12.00 (9.25, 23.50)	19.75 (11.25, 29.00)	31.50 (17.00, 47.25)	44.50 (29.50, 66.25)	<0.001
CCT (μm)	5.00 (2.00, 8.00)	21.00 (11.00, 33.00)	<0.001	12.00 (8.50, 19.50)	17.00 (8.00, 26.00)	26.00 (14.00, 36.75)	29.00 (17.50, 44.75)	<0.001
differential pachymetry (μm)	1.00 (1.00, 2.00)	3.00 (1.88, 5.00)	<0.001	4.00 (2.00, 5.00)	3.00 (1.00, 4.00)	3.00 (1.13, 5.00)	6.00 (2.00, 8.00)	<0.001
Chord_Mu (mm)	0.08 (0.03, 0.13)	0.13 (0.06, 0.23)	<0.001	0.07 (0.02, 0.11)	0.12 (0.04, 0.19)	0.15 (0.08, 0.27)	0.12 (0.07, 0.52)	<0.001
PachyMinX	0.88 (0.55, 1.15)	0.77 (0.50, 1.04)	0.016	0.97 (0.61, 1.19)	0.81 (0.54, 1.11)	0.74 (0.50, 0.97)	0.73 (0.41, 1.03)	0.033
PachyMinY	0.13 (0.06, 0.23)	0.20 (0.09, 0.34)	<0.001	0.15 (0.09, 0.21)	0.20 (0.11, 0.28)	0.20 (0.09, 0.38)	0.27 (0.08, 0.45)	<0.001

Table 3 (continued)

	Normal (n=344)	KC (n=290)	P^a	KC (n=290)				P^b
				KSS 1 (n=16)	KSS 2 (n=100)	KSS 3 (n=136)	KSS 4 (n=38)	
PupilX	0.16 (0.08, 0.28)	0.18 (0.08, 0.32)	0.293	0.19 (0.08, 0.24)	0.15 (0.08, 0.32)	0.19 (0.08, 0.33)	0.23 (0.06, 0.34)	0.752
PupilY	0.09 (0.04, 0.15)	0.16 (0.08, 0.28)	<0.001	0.10 (0.04, 0.16)	0.13 (0.08, 0.24)	0.18 (0.08, 0.34)	0.18 (0.08, 0.41)	<0.001
EccSph	0.03 (0.01, 0.05)	0.22 (0.11, 0.37)	<0.001	0.08 (0.04, 0.19)	0.15 (0.07, 0.27)	0.25 (0.13, 0.40)	0.43 (0.30, 0.54)	<0.001
RMS (Cornea)	0.23 (0.11, 0.40)	5.32 (2.47, 8.76)	<0.001	1.83 (0.79, 2.23)	3.66 (2.21, 5.93)	6.96 (3.14, 10.31)	9.03 (6.60, 14.57)	<0.001
RMS HOA (Cornea)	0.06 (0.03, 0.09)	1.14 (0.50, 1.94)	<0.001	0.41 (0.15, 0.48)	0.78 (0.49, 1.18)	1.62 (0.62, 2.34)	2.21 (1.56, 3.33)	<0.001
RMS LOA (Cornea)	0.23 (0.11, 0.39)	5.15 (2.36, 8.58)	<0.001	1.78 (0.73, 2.18)	3.62 (2.16, 5.84)	6.78 (3.11, 10.04)	8.81 (6.41, 14.25)	<0.001
C.Height (mm)	0.04 (0.02, 0.07)	0.08 (0.03, 0.14)	<0.001	0.05 (0.02, 0.10)	0.06 (0.02, 0.09)	0.10 (0.04, 0.14)	0.16 (0.10, 0.25)	<0.001
C.Volume (mm^3)	5.85 (2.75, 11.28)	7.10 (3.60, 12.33)	0.024	8.25 (5.18, 10.95)	7.1 (3.29, 11.08)	7.15 (3.60, 13.40)	6.60 (2.78, 12.60)	0.184
Cor.Vol. (mm^3)	0.60 (0.20, 1.00)	0.70 (0.30, 1.20)	<0.001	0.75 (0.50, 1.10)	0.50 (0.20, 0.90)	0.85 (0.40, 1.40)	1.10 (0.57, 1.50)	<0.001
Cornea Dia. (mm)	0.10 (0.00, 0.10)	0.10 (0.00, 0.10)	0.207	0.10 (0.10, 0.10)	0.10 (0.00, 0.20)	0.10 (0.00, 0.10)	0.10 (0.08, 0.20)	0.263
Density (%)	0.40 (0.20, 0.70)	0.60 (0.30, 1.00)	<0.001	0.60 (0.23, 0.70)	0.50 (0.30, 0.90)	0.55 (0.30, 0.98)	0.80 (0.48, 1.23)	<0.001
BAD D	0.20 (0.09, 0.33)	4.01 (1.95, 6.71)	<0.001	1.56 (0.59, 2.17)	2.74 (1.59, 4.19)	5.12 (2.60, 7.26)	8.00 (5.37, 9.97)	<0.001

K1, flat keratometry; *K2*, steep keratometry; *Km*, mean keratometry; *K Max*, maximum keratometry; *FEle.Th/B.Ele.Th*, front/back elevation in thinnest location; *RMS*, root mean square; *HOA*, high-order aberration; *LOA*, low-order aberration; *C.Height*, anterior chamber depth measured from the posterior corneal surface to the ocular lens in apex position; *C.Volume*, anterior chamber volume in mm^3 at a diameter of 10 mm around the apex; *Cor.Vol.*, anterior chamber volume in mm^3 at a diameter of 10 mm around the apex; *Cornea Dia.*, corneal diameter; *BAD-D*, Belin/Ambrósio deviation

[a]Mann-Whitney *U* test for intergroup comparison between the normal and KC groups

[b]Kruskal-Wallis *H* test for intergroup comparison between the normal and KC groups divided by KSS

in corneal hysteresis (CH) and corneal resistance factor (CRF) asymmetries was observed in KC stage 4. The abnormality in CH and CRF asymmetries might be attributed to a small number of patients with KC stage 4 or disturbance coming from corneal scar and extreme steep cone in eyes grading at stage 4. But still, this research inspired that interocular asymmetry could be meaningful both morphologically and biomechanically for diagnosis of KC.

The diagnostic performance of interocular asymmetry has been evaluated in several studies, and an agreement of its appreciable value was achieved. Saad et al. [27] reported that with a cutoff value of 0.797 D, the interocular asymmetry in steep K achieved the highest AUC of 0.965, and the sensitivity and specificity was 93.8% and 96.1%, respectively. Henriquez et al. [19] reported that the AUC of interocular asymmetry in PETP was 0.91, with sensitivity of 85%, and specificity of 88%. Dienes et al. [21] reported that with 12 μm as the cutoff value, the AUC of TCT asymmetry was up to 0.99, with 98% sensitivity and 95% specificity. In this study, mean anterior keratometry and maximum anterior keratometry achieve high AUC (>0.95), which is consistent with previous studies. We also found that aberrations perform well in distinguishing normal from KC eyes, especially the higher-order aberrations of the posterior corneal surfaces and the aberrations of the whole cornea (AUC 0.951 and 0.950, respectively), which has not been noticed in previous literatures yet.

Interocular asymmetry also performs well in the diagnosis of early KC. Another study by Henriquez et al. [28] reported that the interocular asymmetry in BAD-D has good ability for distinguishing normal from KC or VEKC (AUC 0.99 and 0.98, respectively). Naderan et al. [20] found the interocular asymmetry in steep K has high AUC of 0.868 with 88.2% sensitivity and 89.5% specificity in distinguishing normal from KCS.

Few researches attempted to establish diagnostic models for KC with interocular asymmetries. Galletti et al. [25] combined five parameters, including mean anterior keratometry, mean posterior keratometry, thinnest pachymetry, front elevation at the thinnest location, and back elevation at the thinnest location, to model a logistic function and a scoring system named intereye asymmetry score. Both diagnostic models showed moderate sensitivity but high specificity, which could help reduce false positive rate. Mehlan et al. [22] also built a logistic diagnostic model mainly utilizing elevation that realized the balance between sensitivity and specificity (0.961 and 0.960, respectively) and performed well in validation set as well. In addition to the calculated parameters reported by the corneal topography, the raw topographic data were also used to quantify the interocular asymmetry in a study by Shen Y et al. [29] and four new-generated parameters (ΔFKmean, ΔFKsd, ΔFEsd, and ΔFEmax) showed the highest AUC of 0.884–0.985.
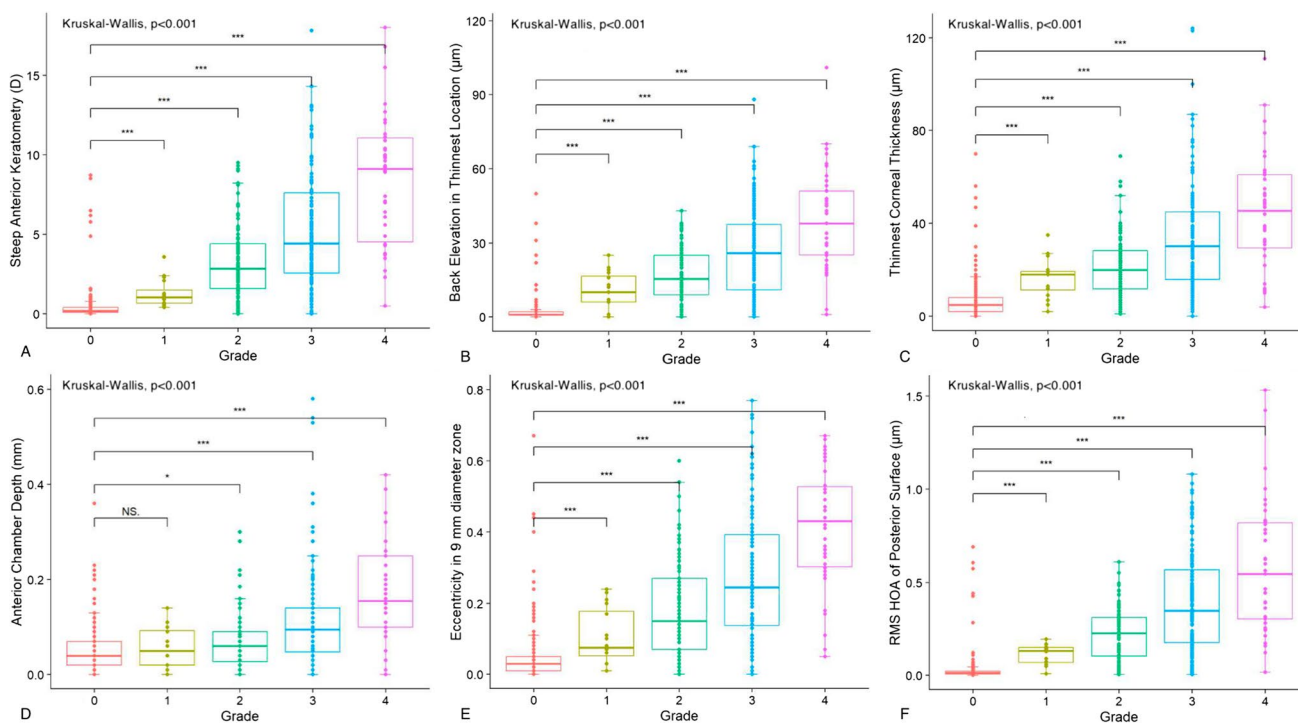

Fig. 1 Box plots showing changes of interocular asymmetry of partial representative parameters with the severity of KC (**A** for steep anterior keratometry, **B** for thinnest corneal thickness, **C** for back elevation in thinnest location, **D** for anterior chamber depth (measured from endothelium), **E** for eccentricity, **F** for root mean square of higher-order aberrations of posterior surface)

Table 4 Diagnostic performance of interocular asymmetry of single parameters and logistic models

	AUC (95% CI)	Cutoff	Sensitivity (%)	Specificity (%)	Accuracy (%)
Anterior surface					
K1 (D)	0.906 (0.880–0.932)	0.650	82.4	94.5	89.0
K2 (D)	0.940 (0.919–0.961)	0.800	88.6	95.3	92.3
Km (D)	0.955 (0.939–0.972)	0.550	90.3	94.5	92.6
K Max (D)	0.953 (0.934–0.972)	1.370	90.0	96.5	93.5
K Max X	0.539 (0.495–0.584)	0.242	62.8	48.8	55.2
K Max Y	0.408 (0.364–0.452)	0.020	96.9	4.1	46.5
Asph. Q F	0.914 (0.889–0.938)	0.115	81.4	94.8	88.6
F.Ele.Th (µm)	0.943 (0.923–0.963)	2.250	88.3	95.6	92.3
RMS (CF)	0.943 (0.921–0.965)	0.841	92.1	94.2	93.2
RMS HOA (CF)	0.947 (0.926–0.967)	0.158	92.1	96.2	94.3
RMS LOA (CF)	0.944 (0.923–0.966)	0.839	91.4	94.2	92.9
Z 3 1 (CF)	0.834 (0.801–0.867)	1.055	66.9	91.0	80.0
Z 3 -1 (CF)	0.925 (0.903–0.947)	0.667	87.6	87.8	87.7
Z 4 0 (CF)	0.908 (0.881–0.936)	0.346	84.8	93.0	89.3
Posterior surface					
K1 (D)	0.909 (0.883–0.934)	0.125	83.4	94.8	89.6
K2 (D)	0.937 (0.916–0.958)	0.150	88.3	92.2	90.4
Km (D)	0.927 (0.904–0.950)	0.150	86.2	96.8	92.0
Asph. Q B	0.887 (0.858–0.916)	0.125	78.3	95.3	87.5
B.Ele.Th (µm)	0.942 (0.922–0.963)	5.500	86.6	95.6	91.5
RMS (CB)	0.947 (0.927–0.967)	0.248	89.7	95.1	92.6
RMS HOA (CB)	0.951 (0.933–0.969)	0.045	90.3	94.2	92.4
RMS LOA (CB)	0.944 (0.924–0.965)	0.248	89.0	94.8	92.1
Z 3 1 (CB)	0.860 (0.827–0.892)	1.801	73.8	95.1	85.3
Z 3 -1 (CB)	0.873 (0.841–0.904)	2.046	76.6	96.2	87.2
Z 4 0 (CB)	0.889 (0.861–0.917)	0.908	77.9	91.3	85.2
Whole cornea					
TCT (µm)	0.895 (0.868–0.922)	12.500	79.0	91.0	85.5
Pachy Apex (µm)	0.907 (0.882–0.932)	11.500	80.7	90.1	85.8
CCT (µm)	0.868 (0.838–0.898)	12.500	72.4	93.3	83.8
differential pachymetry (µm)	0.737 (0.699–0.776)	2.250	59.7	79.4	70.3
Chord_Mu (mm)	0.684 (0.642–0.726)	0.116	61.0	70.1	65.9
PachyMinX	0.444 (0.400–0.489)	0.145	94.8	6.7	47.0
PachyMinY	0.633 (0.590–0.677)	0.155	61.7	60.8	61.2
PupilX	0.524 (0.478–0.570)	0.325	24.8	83.4	56.6
PupilY	0.669 (0.626–0.712)	0.172	46.2	81.1	65.1
EccSph	0.901 (0.874–0.928)	0.080	81.0	92.2	87.1
RMS (Cornea)	0.950 (0.931–0.969)	1.014	88.3	96.2	92.6
RMS HOA (Cornea)	0.939 (0.918–0.961)	0.188	89.7	95.9	93.1
RMS LOA (Cornea)	0.948 (0.929– 0.968)	1.064	87.6	96.8	92.6
C.Height (mm)	0.684 (0.642–0.727)	0.070	55.9	75.3	66.4
C.Volume (mm^3)	0.552 (0.507–0.597)	5.600	60.0	48.8	53.9
Cor.Vol. (mm^3)	0.581 (0.537–0.626)	1.200	30.7	84.9	60.1
Cornea Dia. (mm)	0.522 (0.478–0.565)	0.200	14.5	89.8	55.4
Density (%)	0.605 (0.561–0.649)	0.600	48.3	69.8	59.9
BAD D	0.976 (0.963–0.988)	1.580	95.2	97.4	96.4
BLRI	0.963 (0.945–0.982)	0.303	93.0	95.2	94.1
MLRI	0.963 (0.945–0.981)	0.367	92.5	93.5	93.0
BaLRI	0.971 (0.954, 0.988)	0.295	95.3	97.0	96.2

K1, flat keratometry; *K2*, steep keratometry; *Km*, mean keratometry; *K Max*, maximum keratometry; *F.Ele.Th/B.Ele.Th*, front/back elevation in thinnest location; *RMS*, root mean square; *HOA*, higher-order aberration; *LOA*, lower-order aberration; *C.Height*, anterior chamber depth measured from the posterior corneal surface to the ocular lens in apex position; C.Volume, anterior chamber volume in mm^3 at a diameter of 10 mm around the apex; *Cor.Vol.*, anterior chamber volume in mm^3 at a diameter of 10 mm around the apex; *Cornea Dia.*, corneal diameter; *BAD-D*, Belin/Ambrósio deviation; *BLRI*, binocular logistic regression index, *MLRI*, monocular logistic regression index, *BaLRI*, binocular assisted logistic regression index

Fig. 2 Comparisons of the receiver operating characteristic (ROC) curves of the logistic regression models (BLRI, binocular logistic regression index; MLRI, monocular logistic regression index; BaLRI, binocular-assisted logistic regression index)
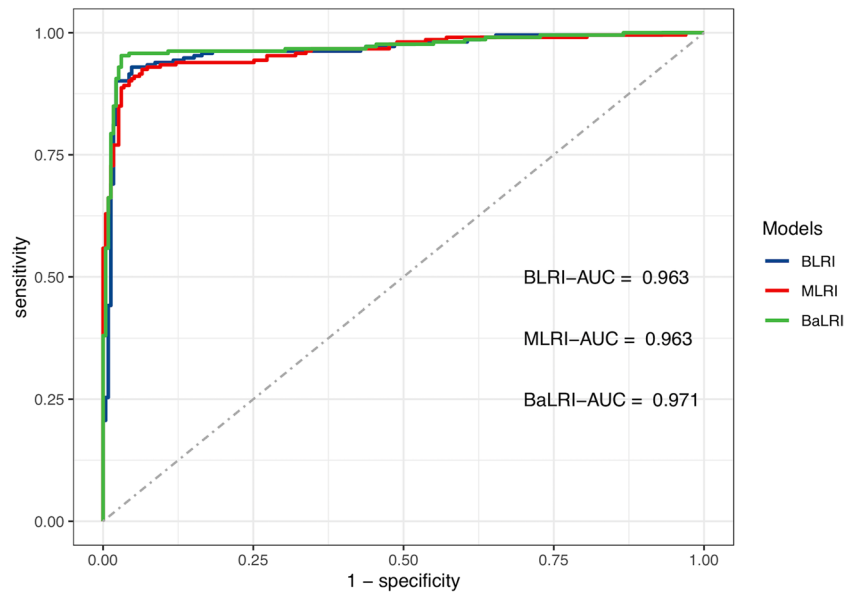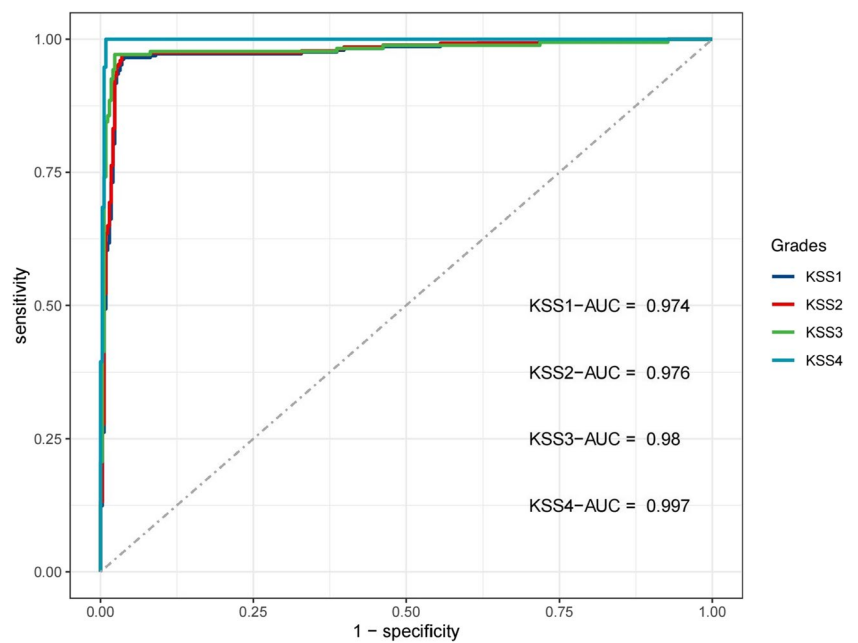
Table 5 The cutoff values of model BaLRI according to the severity of keratoconus

Grading	AUC (95% CI)	Cutoff	Sensitivity (%)	Specificity (%)	Accuracy (%)
KSS 1	0.974 (0.960–0.987)	0.281	96.6	96.2	96.4
KSS 2	0.976 (0.963–0.989)	0.303	97.1	96.5	96.8
KSS 3	0.980 (0.964–0.995)	0.642	97.1	97.7	97.5
KSS 4	0.997 (0.993–1.000)	0.985	100	99.1	99.2

Fig. 3 The ROC curves of model BaLRI according to the severity of keratoconus

We have established a binocular model and a monocular model respectively. Although the binocular model is not significantly superior to the monocular model, the analysis of NRI and IDI shows that interocular asymmetry can indeed bring gain to the monocular model, especially for SKC detection. The sensitivity of BaLRI is higher than that of MLRI, indicating

that the interocular asymmetry might have provided warning information when the monocular parameters are still within the normal range. When applying BaLRI to distinguish between SKC and normal, it showed a trend outperform the classic monocular diagnostic parameter BAD-D. We do not intend to replace monocular diagnostic indicators with the binocular model bluntly, but we realize that incorporating interocular asymmetry can assist existing monocular indicators and achieve more accurate diagnosis of early KC.

There are limitations to present study. First of all, this is a single-center research, although its sample size is not small among similar studies, the analysis of SKC subgroups is still limited. Incorporating more diverse source samples in the future will undoubtedly help improve the model and enhance its robustness. Secondly, this is a retrospective study, and it is better to conduct a longitudinal evaluation of KC in order to find out more quantitative relationship between interocular asymmetry evolution and the severity of disease. Besides, we only used Pentacam Scheimpflug imaging equipment to evaluate the participants. Our results may have systematic errors compared to those based on other corneal topographic equipment, which may affect the promotion and application of interocular asymmetry range obtained in this study.

In conclusion, this study revealed that the interocular asymmetry is significantly different between normal and KC individuals and increases along with the severity. The interocular asymmetry index BLRI proposed in this study can help improve the diagnostic performance of existing monocular indicators. It could serve as an early screening and progression marker for KC to avoid misdiagnosis in false negative patients, thereby improving the safety of corneal refractive surgery. It is worth further exploring the application of interocular asymmetry as a replenishment for monocular descriptors in early diagnosis of KC.

Declarations

References

1. Mintz Y, Brodie R (2019) Introduction to artificial intelligence in medicine. Minim Invasive Ther Allied Technol 28(2):73–81. https://doi.org/10.1080/13645706.2019.1575882

2. Cao K, Verspoor K, Sahebjada S, Baird PN (2022) Accuracy of machine learning assisted detection of keratoconus: a systematic review and meta-analysis. J Clin Med 11(3). https://doi.org/10.3390/jcm11030478

3. Xie Y, Zhao L, Yang X, Wu X, Yang Y, Huang X, Liu F, Xu J, Lin L, Lin H, Feng Q, Lin H, Liu Q (2020) Screening candidates for refractive surgery with corneal tomographic-based deep learning. JAMA Ophthalmol 138(5):519–526. https://doi.org/10.1001/jamaophthalmol.2020.0507

4. Falavarjani KG, Modarres M, Joshaghani M, Azadi P, Afshar AE, Hodjat P (2010) Interocular differences of the Pentacam measurements in normal subjects. Clin Exp Optom 93(1):26–30. https://doi.org/10.1111/j.1444-0938.2009.00446.x

5. Durr GM, Auvinet E, Ong J, Meunier J, Brunette I (2015) Corneal shape, volume, and interocular symmetry: parameters to optimize the design of biosynthetic corneal substitutes. Invest Ophthalmol Vis Sci 56(8):4275–4282. https://doi.org/10.1167/iovs.15-16710

6. Kovács I, Miháltz K, Kránitz K, Juhász É, Takács Á, Dienes L, Gergely R, Nagy ZZ (2016) Accuracy of machine learning classifiers using bilateral data from a scheimpflug camera for identifying eyes with preclinical signs of keratoconus. J Cataract Refract Surg 42(2):275–283. https://doi.org/10.1016/j.jcrs.2015.09.020

7. Zadnik K, Steger-May K, Fink BA, Joslin CE, Nichols JJ, Rosenstiel CE, Tyler JA, Yu JA, Raasch TW, Schechtman KB (2002) Between-eye asymmetry in keratoconus. Cornea 21(7):671–679. https://doi.org/10.1097/00003226-200210000-00008

8. Burns DM, Johnston FM, Frazer DG, Patterson C, Jackson AJ (2004) Keratoconus: an analysis of corneal asymmetry. Br J Ophthalmol 88(10):1252–1255. https://doi.org/10.1136/bjo.2003.033670

9. Nichols JJ, Steger-May K, Edrington TB, Zadnik K (2004) The relation between disease asymmetry and severity in keratoconus. Br J Ophthalmol 88(6):788–791. https://doi.org/10.1136/bjo.2003.034520

10. Ishii R, Kamiya K, Igarashi A, Shimizu K, Utsumi Y, Kumanomido T (2012) Correlation of corneal elevation with severity of keratoconus by means of anterior and posterior topographic analysis. Cornea 31(3):253–258. https://doi.org/10.1097/ico.0b013e31823d1ee0

11. Vinciguerra R, Ambrósio R Jr, Elsheikh A, Roberts CJ, Lopes B, Morenghi E, Azzolini C, Vinciguerra P (2016) Detection of keratoconus with a new biomechanical index. J Refract Surg 32(12):803–810. https://doi.org/10.3928/1081597x-20160629-01

12. Ambrósio R Jr, Lopes BT, Faria-Correia F, Salomão MQ, Bühren J, Roberts CJ, Elsheikh A, Vinciguerra R, Vinciguerra P (2017) Integration of Scheimpflug-based corneal tomography and biomechanical assessments for enhancing ectasia detection. J Refract Surg 33(7):434–443. https://doi.org/10.3928/1081597x-20170426-02

13. Lopes BT, Ramos IC, Salomão MQ, Guerra FP, Schallhorn SC, Schallhorn JM, Vinciguerra R, Vinciguerra P, Price FW Jr, Price MO, Reinstein DZ, Archer TJ, Belin MW, Machado AP, Ambrósio R Jr (2018) Enhanced tomographic assessment to detect corneal ectasia based on artificial intelligence. Am J Ophthalmol 195:223–232. https://doi.org/10.1016/j.ajo.2018.08.005

14. Gomes JA, Tan D, Rapuano CJ, Belin MW, Ambrósio R Jr, Guell JL, Malecaze F, Nishida K, Sangwan VS (2015) Global consensus

on keratoconus and ectatic diseases. Cornea 34(4):359–369. https://doi.org/10.1097/ico.0000000000000408

15. Galletti JD, Ruiseñor Vázquez PR, Fuentes Bonthoux F, Pförtner T, Galletti JG (2015) Multivariate analysis of the ocular response analyzer's corneal deformation response curve for early keratoconus detection. J Ophthalmol 2015:496382. https://doi.org/10.1155/2015/496382

16. Ruiseñor Vázquez PR, Galletti JD, Minguez N, Delrivo M, Fuentes Bonthoux F, Pförtner T, Galletti JG (2014) Pentacam Scheimpflug tomography findings in topographically normal patients and subclinical keratoconus cases. Am J Ophthalmol 158(1):32–40.e2. https://doi.org/10.1016/j.ajo.2014.03.018

17. Henriquez MA, Hadid M, Izquierdo L Jr (2020) A systematic review of subclinical keratoconus and forme fruste keratoconus. J Refract Surg 36(4):270–279. https://doi.org/10.3928/1081597x-20200212-03

18. McMahon TT, Szczotka-Flynn L, Barr JT, Anderson RJ, Slaughter ME, Lass JH, Iyengar SK (2006) A new method for grading the severity of keratoconus: the Keratoconus Severity Score (Kss). Cornea 25(7):794–800. https://doi.org/10.1097/01.ico.0000226359.26678.d1

19. Henriquez MA, Izquierdo L Jr, Mannis MJ (2013) Intereye asymmetry detected by Scheimpflug imaging in subjects with normal corneas and keratoconus. Cornea 32(6):779–782. https://doi.org/10.1097/ICO.0b013e31827b14ae

20. Naderan M, Rajabi MT, Zarrinbakhsh P (2017) Intereye asymmetry in bilateral keratoconus, keratoconus suspect and normal eyes and its relationship with disease severity. Br J Ophthalmol 101(11):1475–1482. https://doi.org/10.1136/bjophthalmol-2016-309841

21. Dienes L, Kránitz K, Juhász E, Gyenes A, Takács A, Miháltz K, Nagy ZZ, Kovács I (2014) Evaluation of intereye corneal asymmetry in patients with keratoconus. A Scheimpflug Imaging Study. PLoS One 9(10):e108882. https://doi.org/10.1371/journal.pone.0108882

22. Mehlan J, Steinberg J, Druchkiv V, Katz T, Linke SJ (2022) Topographic, tomographic, and corneal wavefront asymmetry in keratoconus: towards an eye asymmetry index Easix. Graefes Arch Clin Exp Ophthalmol 260(9):2949–2958. https://doi.org/10.1007/s00417-022-05642-5

23. Xu G, Hu Y, Zhu S, Guo Y, Xiong L, Fang X, Liu J, Zhang Q, Huang N, Zhou J, Li F, Lei X, Jiang L, Wang Z (2021) A multicenter study of interocular symmetry of corneal descriptors in Chinese myopic patients. Sci Rep 11(1):5536. https://doi.org/10.1038/s41598-021-84937-9

24. Bussières N, Ababneh OH, Abu Ameerh MA, Al Bdour MD (2017) Keratoconus asymmetry between both eyes based on corneal tomography. Middle East Afr J Ophthalmol 24(4):171–176. https://doi.org/10.4103/meajo.MEAJO_311_16

25. Galletti JD, Ruiseñor Vázquez PR, Minguez N, Delrivo M, Bonthoux FF, Pförtner T, Galletti JG (2015) Corneal asymmetry analysis by Pentacam Scheimpflug tomography for keratoconus diagnosis. J Refract Surg 31(2):116–123. https://doi.org/10.3928/1081597x-20150122-07

26. Eppig T, Spira-Eppig C, Goebels S, Seitz B, El-Husseiny M, Lenhart M, Papavasileiou K, Szentmáry N, Langenbucher A (2018) Asymmetry between left and right eyes in keratoconus patients increases with the severity of the worse eye. Curr Eye Res 43(7):848–855. https://doi.org/10.1080/02713683.2018.1451545

27. Saad A, Guilbert E, Gatinel D (2014) Corneal enantiomorphism in normal and keratoconic eyes. J Refract Surg 30(8):542–547. https://doi.org/10.3928/1081597x-20140711-07

28. Henriquez MA, Izquierdo L Jr, Belin MW (2015) Intereye asymmetry in eyes with keratoconus and high ammetropia: Scheimpflug imaging analysis. Cornea 34(Suppl 10):S57–S60. https://doi.org/10.1097/ico.0000000000000608

29. Shen Y, Xian Y, Han T, Wang X, Zhou X (2021) Bilateral differential topography-a novel topographic algorithm for keratoconus and ectatic disease screening. Front Bioeng Biotechnol 9:772982. https://doi.org/10.3389/fbioe.2021.772982

Authors and Affiliations

Ruilan Dong[1,2,3] · Yan Liu[1,2,3] · Yu Zhang[1,2,3] · Yueguo Chen[1,2,3]

✉ Yueguo Chen
chenyueguo@263.net

1. Department of Ophthalmology, Peking University Third Hospital, 49 North Garden Road, Haidian District, Beijing 100191, China

2. Beijing Key Laboratory of Restoration of Damaged Ocular Nerve, Peking University Third Hospital, Beijing, China

3. Peking University Institute of Laser Medicine, Beijing, China